PILOT OPTICAL ALIGNMENT AND ITS IN FLIGHT PERFORMANCES

B. Mot[1], Y. Longval[4], P. Ade[2], Y. André[3], J. Aumont[4], L. Baustista[3], J.-Ph. Bernard[1], N. Bray[3], P. de Bernardis[7], O. Boulade[5], F. Bousquet[3], M. Bouzit[4], V. Buttice[4], A. Caillat[4], M. Charra[4], M. Chaigneau[4], C. Coudournac[3], B. Crane[4], J.-P. Crussaire[4], F. Douchin[3], E. Doumayrou[5], J.-P. Dubois[4], C. Engel[1], P. Etcheto[3], P. Gélot[3], M. Griffin[2], G. Foenard[1], S. Grabarnik[6], P. Hargrave[2], A. Hughes[1], R. Laureijs[6], Y. Lepennec[5], B. Leriche[4], S. Maestre[1], B. Maffei[4], J. Martignac[5], C. Marty[1], W. Marty[1], S. Masi[7], F. Mirc[3], R. Misawa[1], J. Montel[3], L. Montier[1], J. Narbonne[1], J-M. Nicot[3], F. Pajot[1], G. Parot[3], E. Pérot[8], J. Pimentao[7], G. Pisano[2], N. Ponthieu[9], I. Ristorcelli[1], L. Rodriguez[5], G. Roudil[1], M. Salatino[7], G. Savini[2], O. Simonella[3], M. Saccoccio[3], P. Tapie[3], J. Tauber[6], J.-P. Torre[4], C. Tucker[2], and G. Versepuech[1]

[1] IRAP, Institut de Recherche en Astrophysique et Planétologie, CNRS, 9 Avenue du Colonel Roche, BP 44346, 31028 Toulouse, France

[2] Department of Physics and Astrophysics, Cardiff University, the Parade, Cardiff CF24 3AA, UK

[3] Centre National des Etudes Spatiales, DCT/BL/NB, 18 Av. E. Belin, 31401 Toulouse, France

[4] Institut d'Astrophysique Spatiale, CNRS, Univ. Paris-Sud, Univ. Paris-Saclay, Bât. 121, 91405 Orsay cedex, France

[5] CEA/Saclay, 91191 Gif-sur-Yvette Cedex, France

[6] Scientific Support Office, SRE-S, ESTEC, PO Box 299,2200AG Noordwijk, The Netherlands

[7] Universita degli studi di Roma "La Sapienza", Dipartimento di Fisica, P.le A. Moro, 2, 00185, Roma, Italia

[8] Thales Services, Toulouse, France

[9] Institut de Planétologie et d'Astrophysique de Grenoble, Université Grenoble Alpes, Bât OSUG A, CS 40700, 38058 Grenoble Cedex 9, France

I. INTRODUCTION

PILOT (Polarized Instrument for Long wavelength Observations of the Tenuous interstellar medium) is a balloon-borne astronomy experiment designed to study the polarization of dust emission in the diffuse interstellar medium in our Galaxy[1,2]. The PILOT instrument allows observations at wavelengths 240 μm (1.2THz) with an angular resolution about two arc-minutes. The observations performed during the first flight in September 2015 at Timmins, Ontario Canada, have demonstrated the optical performances of the instrument.

Pilot optics is composed an off axis Gregorian type telescope, a refractive re-imager and polarimeter system. All optical elements are in a cryostat cooled to 3K except the primary mirror, which is at ambient temperature (the room temperature during the end-to-end ground test or the temperature at ceiling altitude ~ 40 km in flight).

All optics system is aligned at room temperature and we have developed a dedicated procedure in order to keep the tight requirements on the focus position and ensure the instrument performances in the different environments. We combined the optical, 3D dimensional measurement methods and thermoeslastic modeling to perform the optical alignment.

The talk describes the system analysis, the alignment procedure, and finally the performances obtained during end-to-end ground test and the first flight.

II. OPTICAL ALIGNMENT METHODOLOGY

A. PILOT Optics description

The PILOT optics is composed of three major parts: a telescope, a re-imager and a polarimeter. Fig.1 shows the optical layout through the overall system.

The telescope is of tilted Gregorian type, composed of three mirrors. The primary M1 is an off-axis parabolic mirror with a projected aperture of 830 mm, while the secondary M2 is an off-axis elliptical mirror. The combination of M1 and M2 fulfills the Mizuguchi-Dragone condition to form an equivalent on-axis parabolic telescope minimizing the instrumental polarization effect [3,4]. The third mirror M3 is flat to fold the beam onto the re-imaging refractive optics. All mirrors and their mounts are made of aluminum to reduce thermo-elastic effects that will affect the image quality.

The re-imager conjugates the telescope focal plane onto the detectors through a telecentric optics formed by lenses L1 and L2, made of polypropylene material. It is optimized to make the cold optics less sensitive to thermo-elastic

effects of the photometer and to get diffraction limited image quality. The lens L1 conjugates the primary mirror M1 aperture onto the cold-stop (Aperture Stop) to block the stray light coming from M1 edge diffraction.

The polarimeter is composed by a rotating Half-Wave-Plate and a polarizer in order to measure the incoming beam's Stokes parameters. The HWP is located just before the Cold-Stop. The polarizer acts as also a beamsplitter, which separates the beam into two, one is transmitted on the Transmission Detection Arrays and the other is reflected on the Reflection Detection Arrays. The two beams have two orthogonal linear polarizations.

To obtain the diffraction limited image quality, the telescope alignment is the most stringent among the three optical parts. All optical components except the primary mirror M1 are cooled at 3K, located inside a cryostat (the Photometer). So for the telescope, M1 is at ambient temperature, M2 and M3 are at cold temperature 3K. We describe below the alignment of the Primary mirror with the photometer performed for room temperature for the end-to-end test and for stratospheric flight observation.
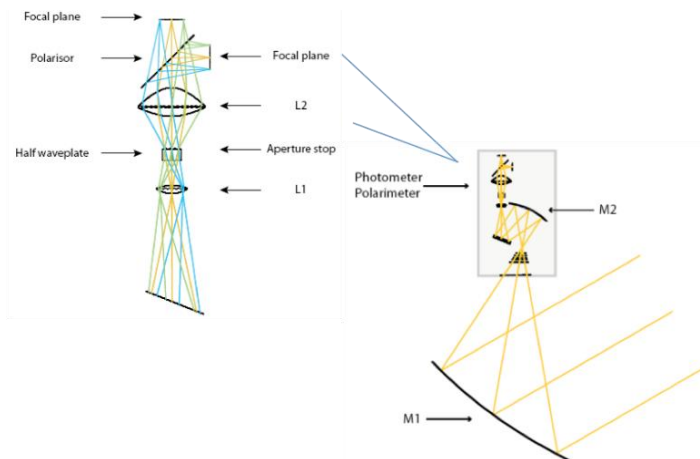

Fig. 1. PILOT Optical Layout. Only the M1 mirror is located outside the photometer.

B. Alignment Requirement

Zemax software has been used to analyze the sensitivity to the positioning of each component, and has shown that the telescope (mirrors M1, M2 and M3) alignment is the most critical, and therefore the alignment between M1 and the photometer (containing M2 and M3 which are cold) is of prime importance.

In order to obtain the diffraction limited image quality at 240µm, the primary mirror and the secondary mirror focal points, M1_F1 and M2_F1 (see **Fig. 2**), should be within a position tolerance of 0.6 mm along each of the axis, their symmetrical plane and their main optical axis should be aligned within an angle of 0.06°.
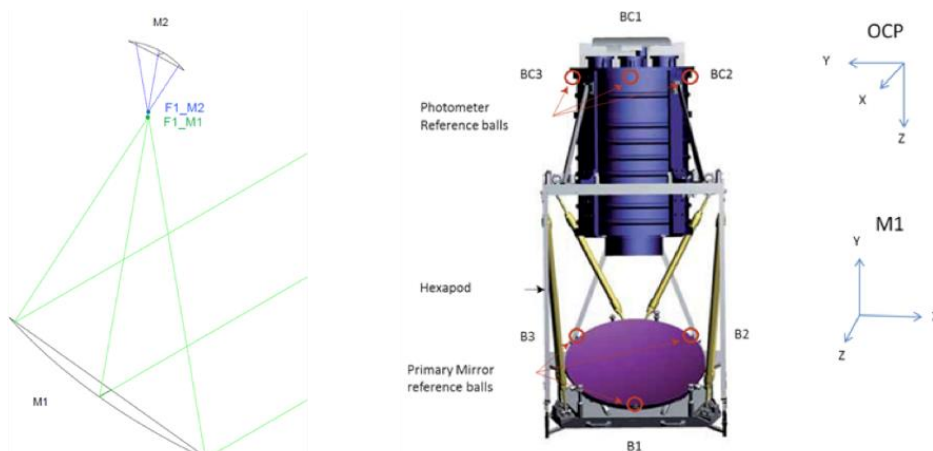

Fig. 2. Photometer and M1 alignment.

This requirement must be satisfied at any time during the observations at ceiling altitude, while the elevation of the pointed payload is changed and the temperature of the structure evolves, producing thermo-elastic deformation. This is actually one of the most stringent requirements for the experiment.

C. Alignment Philosophy

To fulfill this requirement, a series of actions has been performed: First, precise characterizations of the optical and mechanical properties of the primary mirror and of the photometer have been carried out separately [10]. Second, specific tools and an efficient procedure have been developed to align the two subsystems, both for ground test and flight observations.

The M1 mirror characterization was performed with the help of the IRAP submillimeter test bench using a 1m-diameter collimator with 5340 mm focal length. A dedicated methodology, based on optical and 3D measurements were developed for this characterization [5,7].

The cold optical component geometric characteristics were determined at room temperature. The material thermoelastic coefficients (TEC) are measured down to 4K (aluminum and polypropylene). Then the optimizations are proceeded with Zemax software taking into account the optical properties and thermoelastic effects. The secondary mirror M2 is an off-axis elliptical mirror, its optical properties were measured by means of optical interferometer and their two focal point positions were obtained using 3D measurement by Faro-Arm.

The positioning of the cold optics was provided by Zemax modeling, based on ambient temperature characterization of the cold optics (M2, M3, L1, L2) and on a thermo-elastic study. This optical alignment was first checked by means of a dedicated IAS test bench. This bench is composed of a modulated blackbody source, a focusing lens (consistent with PILOT optics) and of a flat fold mirror [6].

Two coordinate systems have been used (see **Fig. 2**) during subsystem tests and alignment:
  1. M1 coordinate system represented by three reference balls B1, B2 and B3
  2. Photometer coordinate system, Ocp, represented by BC1, BC2 and BC3.
All optical subsystem properties are measured at their coordinate system. And then the two subsystems are attached to the fixed platform (see **Fig. 3** left). The fixed platform is the reference base of the instrument.

To perform the whole instrument alignment, the primary mirror position is adjustable. It was mounted on a hexapod allowing six degrees of freedom adjustments, at the same time; it maintains the stiffness of the system. A numerical model of this mechanism allowed for a fast convergence of the optical alignment (see **Fig. 3** right).
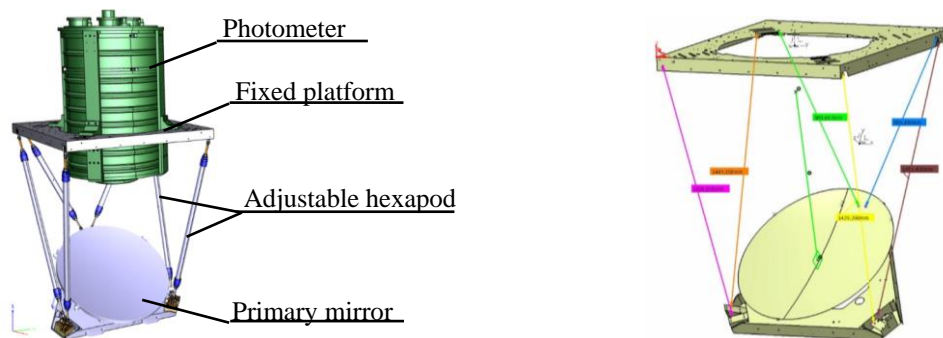

Fig. 3. Schematic view of the hexapod system (left) and its modeling (right).

We used a Leica laser tracker system to get the relative position of the two subsystems (M1 and photometer) by measuring the positions of the two groups of reference balls B1, B2, B3 and BC1, BC2, BC3. See the Fig. 2.

The Leica Laser Tracker system (see **Fig. 4**) is composed of a distance meter, an interferometer, a stabilized HeNe laser (632.8nm), an infrared laser and of a camera (T-Cam). The laser tracker measures the position of a Tooling ball center in relation with its mechanical references. The specific tooling ball reflectors (TBR) are used for our reference balls. The associated software Spatial Analyser is used to perform the data processing. We developed a specific procedure to allow us to adjust the hexapod efficiently to reach the telescope alignment requirement.

The measurement accuracy depends on the distance between the laser tracker and the TBR, and it is expressed as $\pm 10 \, \mu m + 5 \, \mu m/m$. For PILOT measurements, the overall uncertainty is estimated about 30µm, it is good enough for the requirement.
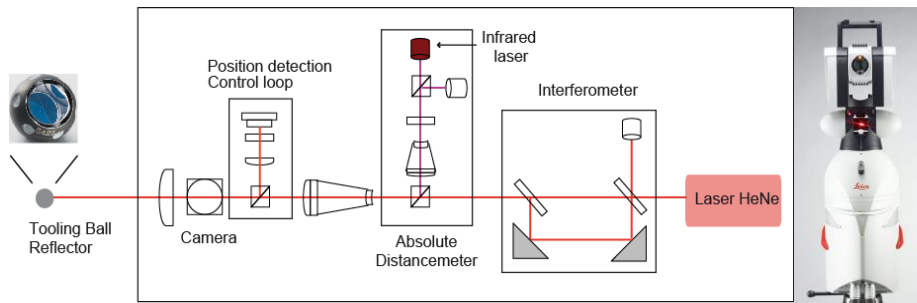
Fig. 4. Left: Schematic view of the LaserTracker system. Right: Laser tracker equipped with its Camera that allows measurements with T-Probe and T-Scan systems.

In order to set the optical alignment for the flight, a thermo-mechanical model of the instrument has been developed. Knowing the temperature at ceiling altitude, this model has been used to predict the displacement due to thermal contractions between ground and operational conditions. Corrections have been applied accordingly before launch, compensating to first order the effect of the thermal expansion of the mechanical structure expected at ceiling altitude.

Furthermore, the deformations of the mechanical structure due to gravity at the various elevations have been modeled using the finite element analysis method with Nastran software. These deformations are expected to be somewhat lower than thermal deformations. They have also been measured during the end-to-end ground tests.

III. PILOT GROUND CONFIGURATION ALIGNMENT

The nominal positioning of the primary mirror and the photometer was obtained by a Zemax modeling, based on ambient temperature characterization of the optical subsystems.
During the PILOT performance tests campaign [2, 8, 9], we did a series of defocusing between the primary mirror and the photometer around the best-estimated focus (see **Fig. 5**). These systematic explorations were performed along three orthogonal axes within typically ±0.8 mm along X and Y axis, and ±1.6 mm along Z axis with a pitch about 0.2 mm (Z is along the optical axis of the photometer, X is included in the optical symmetry plane).
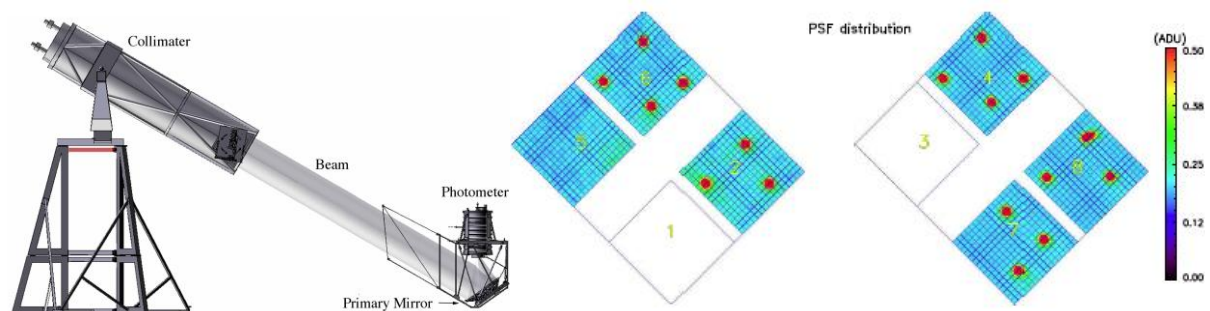

Fig. 5. Left: schematic view of the IRAP sub-mm bench configured for the PILOT tests. The collimator generates a 1m collimated beam, it is located on the top of a tower that allows to modify the inclination of the beam. Right: Defocusing test, distribution of the collimated source position on the pilot focal plane.

For each defocus position, a collimated source was positioned at different location in the focal plane as shown in **Fig. 5**. In order to estimate the impact of defocusing on the optical performances, we measured the PSF image by microscanning and compared the changes by the Full Width Half Maximum (FWHM) as criteria. The following **Fig. 6** shows the measured FWHM as a function of defocusing distance on the array #2.
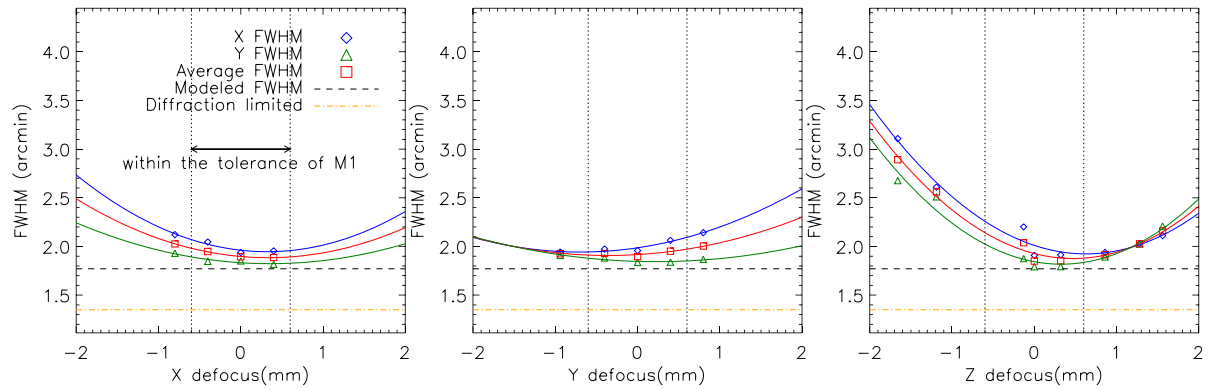
Fig. 6. Example of measured FWHM (on the array #2) as a function of defocusing distance along the X axis (left), Y axis (center), Z axis (right). For each axis, a defocus of 0mm corresponds to the best theoretical focus.

We noticed that the defocus effect along the Z-axis is more sensitive than those along the X and Y axis. The best focus position was set at the position of minimum FWHM of PSF. The best focus position is at X=0, Y=0 and Z=0.2mm. The PSF obtained for this position is shown in **Fig. 7**.
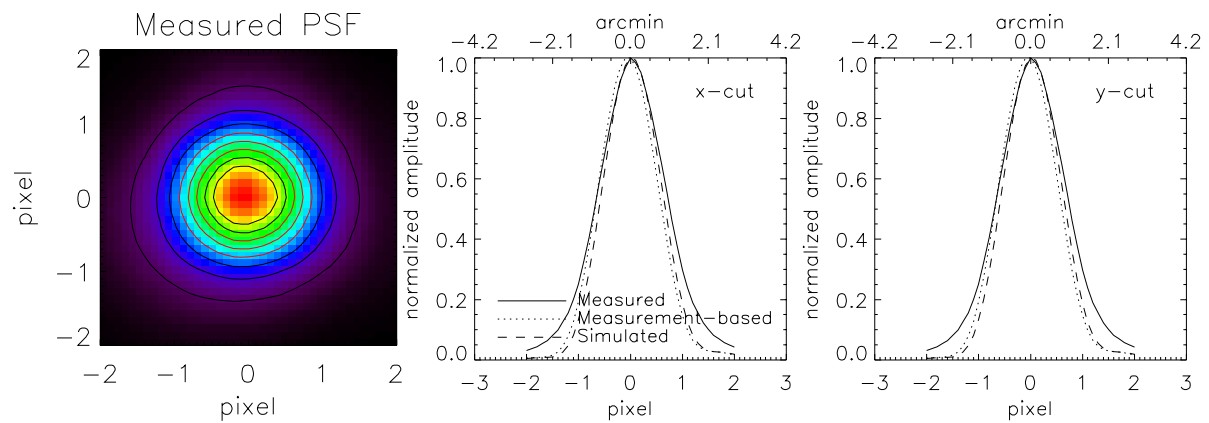

Fig. 7. Measured PSF at the best focus position. Left: The image of the PSF is obtained from a micro-scanning pattern on a 2x2 pixels region on the array #6. Center & right: The X (center) and Y(right) normalized cuts across the measured PSF.

IV. PILOT FLIGHT CONFIGURATION ALIGNMENT

A. Analysis and Method

Because of the temperature gradient between the primary mirror (at ambient temperature) and the cold optics (temperature regulated to 3K), the PILOT telescope thermal deformation is not homothetic. In addition, the electronics power and the Sun radiations generate a temperature gradient within the mechanical structure of the instrument.

The alignment for the flight configuration must take into account thermo-elastic deformations of the mechanical structure and of the optical subsystems. A thermal model of the PILOT gondola has been developed by CNES, it predicted, for a nominal flight, the temperature evolution of the various elements of the PILOT telescope.
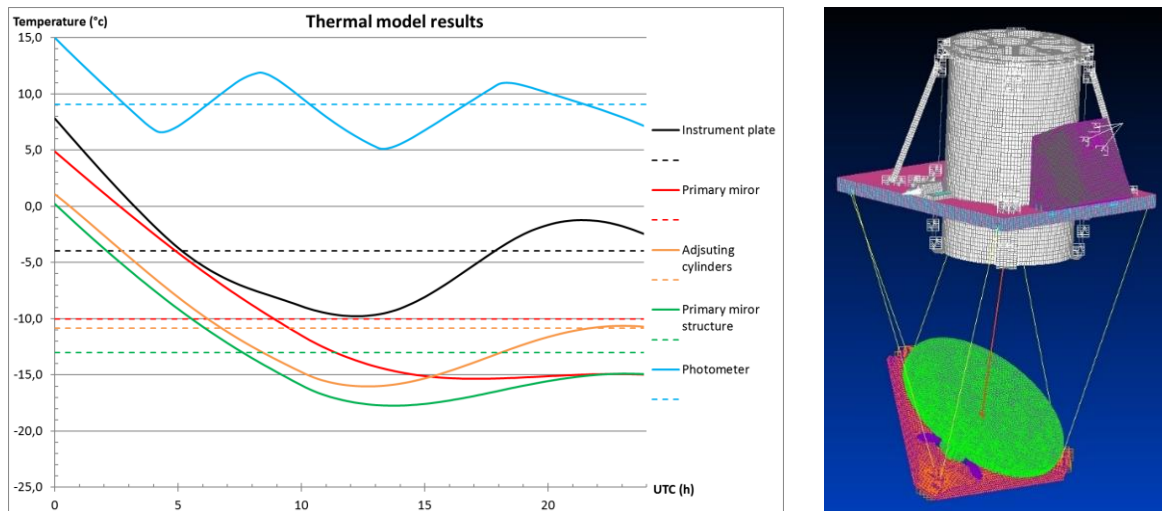
Fig. 8. On the left: Estimated temperature for the main elements of the telescope (dashed lines are average temperatures) based on the CNES thermal modeling (ceiling altitude reached at 0h UTC). On the right: Thermo-elastic deformation modeling of the PILOT telescope based on a finite element study.

The thermo-elastic model (see **Fig. 8**), using FEMAP NASTRAN software, gives an estimate of the defocus that would be due to the thermal effect. Taking into account the average temperature predicted by the thermal model for each elements of the PILOT telescope, the expected defocusing is about 1.06 mm on the Z axis and 0.68 mm on the Y axis. The alignment performed for the flight took into account this defocusing in order to obtain the best focus position during the flight.

B. Flight results and analysis

During the first flight, the average temperatures of the main elements of the telescope were approximatively as predicted by the thermal model (see **Fig.** 9).
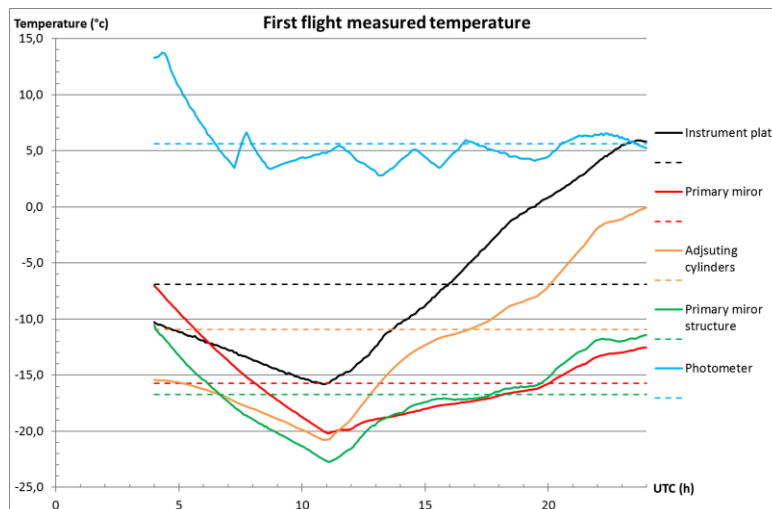

Fig. 9. Measured temperature during the first flight for the main elements of the telescope, dashed lines are average temperatures (ceiling altitude reached at 4h UTC).

During the first flight, we pointed the telescope on planet Saturn, assumed to be a sub-mm point source. These observations have allowed us to check the PILOT optical performances. The following **Fig. 10** shows the images of Saturn seen by each array (left), and the latitude and longitude cuts of the image (right).

The FWHM of the images is about 2.1 arcmin. These images of Saturn obtained during the first flight demonstrated the optical quality was consistent with ground calibration data.
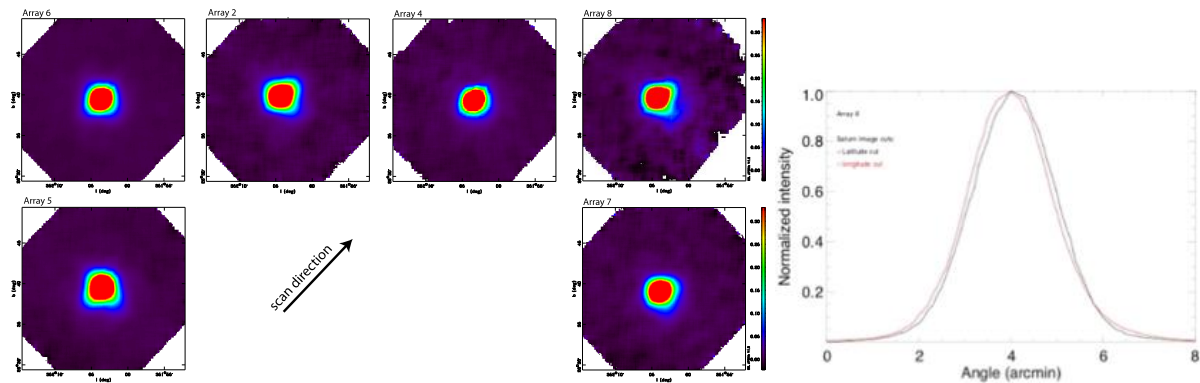
Fig. 10. Left: Images from Saturn obtained during the first flight. Each image is normalized to its peak value. The arrow shows the scan direction. **Right:** Latitude and longitude cuts of the Saturn image on array 6.

C. Flight alignment post-processing

A thermo-elastic model of the PILOT telescope in its first flight configuration has been developed by IRAP. This model takes into account the measured temperature of the main elements of the PILOT telescope during the whole flight.
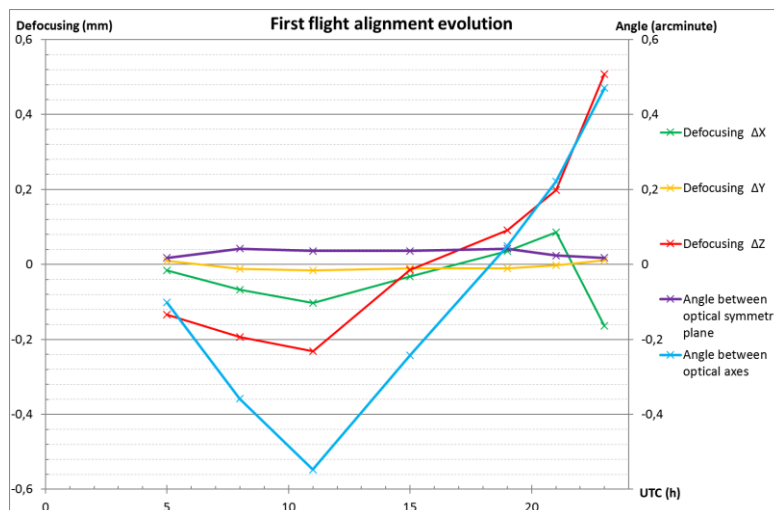

Fig.11. PILOT telescope optical alignment evolution during the first flight (ceiling altitude reached at 4h UTC). Defocusing are defined in the photometer coordinate system, the angle between optical symmetry planes is a rotation around Z axis from X in the photometer coordinate system (other rotations are not significant) and the angle between optical axes is a rotation around Y axis from Z in the photometer coordinate system (other rotations are not significant).

The defocus was always smaller than 0.16 mm on the X axis, 0.02 mm on the Y axis and 0.51 mm on the Z axis. The tilted angle between optical axis was smaller than 0.55 arcminutes and smaller than 0.04 arcminutes for the optical symmetry planes.

All these deviations were within the alignment requirement (see chapter II.*B*)**:** displacement along all axis within 0.6mm and tilts angle within 0.06°.

With these results, the image quality evolution has been estimated with the optical model of the telescope (using Zemax software). The **Fig. 12** shows the Strehl ratio and the PSF evolution by Ellipticity during the first flight. The ellipticity is defined here as the ratio of maximum FWHP over minimum FWHP by supposing the beam PSF pattern is of elliptical shape.
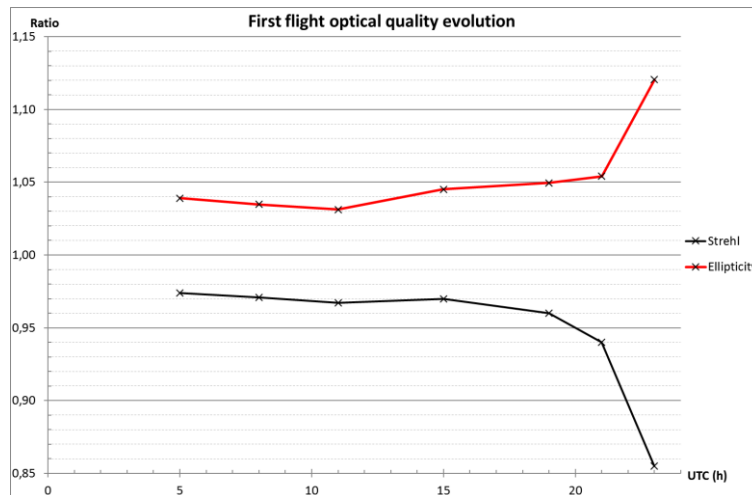
Fig.12. PILOT telescope optical quality (Strehl ratio in black & PSF beam ellipticity in red) evolution during the first flight (ceiling altitude reached at 4h UTC).

V. CONCLUSION

PILOT is a balloon-born astronomy experiment with its specific complexity of optics and observation environment, the first flight at Timmins, Ontario Canada in September 2016 has been successful and data analysis is on-going.

We presented how a combination of optical characteristics provided from ground calibration data, together with some optical and thermo-mechanical modeling allowed us to achieve the optical alignment requirements, both for ground tests, in a controlled environment, and for flight configurations with its uncertainties.

The flight data analysis has shown that the PILOT optical alignment is successful and its optical quality was compliant with the specifications during the first flight. That has been achieved thanks to the alignment methods developed to estimate, characterize and to compensate for the thermo-elastic effects.

REFERENCES

[1]   Bernard, J.-P. and the PILOT team, "PILOT: a balloon-borne experiment to measure the polarized FIRemission of dust grains in the interstellar medium," Exp. Astronomy.
[2]   Misawa, R. and the PILOT team, "PILOT optical performances from ground end-to-end tests," Exp. Astronomy.
[3]   C. Dragone, IEEE Trans. Ant. Prop. AP-30,331, 1982.
[4]   Y. Longval, J-P Bernard, I. Ristorceli, F. Pajot and the PILOT team, "PILOT: optical performance and end-to-end characterization", Proc. ICSO(2014).
[5]   C. Engel, I. Ristorcelli, J-P. Bernard, Y. Longval, C. Marty, B. Mot, G. Otrio, and G. Roudil, "Characterization and performances of the primary mirror of the PILOT balloon-borne experiment," Experimental Astronomy 36, 21–57 (Aug. 2013).
[6]   V. Buttice, Caractérisation et étalonnage de la caméra de l'expérience ballon PILOT (Polarized Instrument for Long wavelength Observation of the Tenuous interstellar medium) Ph.D. thesis Université Paris 11 (2013).
[7]   B. Mot, Assemblage, Intégration et Tests de l'instrument scientifique PILOT (Polarized Instrument for Long wavelength Observation of the Tenuous interstellar medium) Master.D. thesis, Conservatoire National des Arts et Métiers (2011).
[8]   R. Misawa, J-Ph. Bernard and the PILOT team "PILOT: a balloon-borne experiment to measure the polarized FIR emission of dust grains in the interstellar medium" Proc. SPIE(2014).
[9]   R. Misawa, J-Ph. Bernard and the PILOT team, "PILOT end-to-end calibration results", Proc. ESA Rocket Balloon(2015).
[10]   Y. Longval, B. Mot and the PILOT team, "Pilot optical alignment", Proc. SPIE(2016) to be published.